Table 1. Atopic eczema case–control association analysis for *FLG* null variants in Japan

	R501X		3321delA		S1695X		Q1701X		S2554X		S2889X		S3296X		K4022X		Combined			
Genotype	Con	AE	Con	AE	Con	AE	Con	AE	Con	AE	Con	AE	Con	AE	Con	AE	Con	AE (total)	AE (asthma+)	AE (asthma−)
AA	134	172	133	163	133	172	134	169	133	162	132	152	134	166	134	169	129	126	53	73
Aa	0	0	1	9	1	0	0	3	1	10	2	20	0	6	0	3	5	41	18	23
aa	0	0	0	0	0	0	0	0	0	0	0	0	0	0	0	0	0	5[1]	2	3
Total	134	172	134	172	134	172	134	172	134	172	134	172	134	172	134	172	134	172	73	99

Abbreviations: AE, atopic eczema; CI, confidence interval; Con, healthy control; OR, odds ratio.
For combined genotype: AE+asthma, exact *P*-value of Pearson χ^2-test=1.909×10^{-6}, OR and 95% CI for dominant models (AA vs aX)=9.737 (3.473–27.322); AE−asthma, exact *P*-value of Pearson χ^2-test=7.189×10^{-7}, OR and 95% CI for dominant models (AA vs aX)=9.191 (3.383–24.938); all AE, exact *P*-value of Pearson χ^2-test=1.189×10^{-7}, OR and 95% CI for dominant models (AA vs aX)=9.416 (3.625–24.450).
[1]All the five patients were compound heterozygotes for minor alleles.

Table 2. Asthma case–control association analysis for *FLG* null variants in Japan

	R501X		3321delA		S1695X		Q1701X		S2554X		S2889X		S3296X		K4022X		Combined			
Genotype	Con	Asthma	Con	Asthma	Con	Asthma	Con	Asthma	Con	Asthma	Con	Asthma	Con	Asthma	Con	Asthma	Con	Asthma (total)	Asthma (AE+)	Asthma (AE−)
AA	134	137	133	137	133	137	134	137	133	133	132	132	134	136	134	136	129	126	14	112
Aa	0	0	1	0	1	0	0	0	1	4	2	5	0	1	0	1	5	11	4	7
aa	0	0	0	0	0	0	0	0	0	0	0	0	0	0	0	0	0	0	0	0
Total	134	137	134	137	134	137	134	137	134	137	134	137	134	137	134	137	134	137	18	119

Abbreviations: AE, atopic eczema; CI, confidence interval; Con, healthy control; OR, odds ratio.
For combined genotype: asthma+AE, exact *P*-value of Pearson χ^2-test=0.0122, OR and 95% CI for dominant models (AA vs aX)=7.3692 (1.7715–30.6748); asthma−AE, exact *P*-value of Pearson χ^2-test=0.5563, OR and 95% CI for dominant models (AA vs aX)=1.6124 (0.4979–5.2219); all asthma, exact *P*-value of Pearson χ^2-test=0.1968, OR and 95% CI for dominant models (AA vs aX)=2.2523 (0.7609–6.6667).

observed in our Japanese controls was only 3.7%, which was much lower than that seen in European general population, where it is approximately 7.5%. This suggested that there may be further mutations yet to be discovered in the Japanese. As we have sequenced more than 40 Japanese families with ichthyosis vulgaris, there is now little possibility that further highly prevalent mutations will be found in the Japanese population. However, it is still possible that there might be multiple, further low-frequency *FLG* mutations discovered in the Japanese population. In addition, because of the relatively small sample size of this genetic study, further replication in association studies will be required for *FLG* mutations and asthma in Japan.

In our cohorts, serum IgE levels were extremely high (median, 3141.9 IU ml^{-1}; 25th–75th percentiles, 1276.0–9753.0 IU ml^{-1}) in AE patients with asthma ($n=73$) in the AE cohort, compared with that in total asthma patients (median, 156.0 IU ml^{-1}; 25th–75th percentiles, 71.05–441.45 IU ml^{-1}, $n=137$) in the asthma cohort. These findings suggest that extrinsic allergic sensitization might have an important role in atopic asthma pathogenesis. Recent studies hypothesized skin barrier defects caused by *FLG* mutation(s) allow allergens to penetrate the skin, resulting in initiation of further immune response and leading to the development of systemic allergies, including atopic asthma (Fallon *et al.*, 2009). In patients with asthma that also harbor *FLG* mutations, we could not exclude the possibility that the systemic effects of early eczema might simply influence airway responsiveness (Henderson *et al.*, 2008).

CONFLICT OF INTEREST

Irwin McLean has filed patents relating to genetic testing and therapy development aimed at the filaggrin gene.

ACKNOWLEDGMENTS

We thank the patients and their families for their participation. We also thank Kaori Sakai for fine technical assistance and Dr James McMillan for proofreading and comments concerning this paper. This work was supported in part by Grants-in-Aid from the Ministry of Education, Science, Sports, and Culture of Japan to M Akiyama (Kiban B 20390304) and by the Health and Labour Sciences Research Grant (Research on Allergic Diseases and Immunology; H21-Meneki-Ippan-003) to H Shimizu. Filaggrin research in the McLean laboratory was supported by grants from The British Skin Foundation; The National Eczema Society; The Medical Research Council (Reference number G0700314); A*STAR, Singapore, and donations from anonymous families affected by eczema in the Tayside region of Scotland.

Rinko Osawa[1], Satoshi Konno[2], Masashi Akiyama[1], Ikue Nemoto-Hasebe[1], Toshifumi Nomura[1,3], Yukiko Nomura[1], Riichiro Abe[1], Aileen Sandilands[3], W.H. Irwin McLean[3], Nobuyuki Hizawa[4,5], Masaharu Nishimura[2] and Hiroshi Shimizu[1]

[1]Department of Dermatology, Hokkaido University School of Medicine, Sapporo, Japan; [2]First Department of Medicine, Hokkaido University School of Medicine, Sapporo, Japan; [3]Epithelial Genetics Group, Division of Molecular Medicine, University of Dundee, Colleges of Life Sciences and Medicine, Dentistry & Nursing, Dundee, UK;

[4]*Department of Pulmonary Medicine, Institute of Clinical Medicine, Graduate School of Comprehensive Human Sciences, University of Tsukuba, Tsukuba, Ibaraki, Japan and* [5]*University Hospital, University of Tsukuba, Tsukuba, Ibaraki, Japan*
E-mail: akiyama@med.hokudai.ac.jp

REFERENCES

Fallon PG, Sasaki T, Sandilands A *et al.* (2009) A homozygous frameshift mutation in the mouse *Flg* gene facilitates enhanced percutaneous allergen priming. *Nat Genet* 41: 602–8

Hanifin JM, Rajka G (1980) Diagnostic features of atopic dermatitis. *Acta Derm Venereol* 92:44–7

Henderson J, Northstone K, Lee SP *et al.* (2008) The burden of disease associated with filaggrin mutations: a population-based, longitudinal birth cohort study. *J Allergy Clin Immunol* 121:872–7

Isada A, Konno S, Hizawa N *et al.* (2010) A functional polymorphism (-603A —> G) in the tissue factor gene promoter is associated with adult-onset asthma. *J Hum Genet* 55: 167–74

Nemoto-Hasebe I, Akiyama M, Nomura T *et al.* (2010) *FLG* mutation p.Lys4021X in the C-terminal imperfect filaggrin repeat in Japanese atopic eczema patients. *Br J Dermatol* 161:1387–90

Nomura T, Akiyama M, Sandilands A *et al.* (2008) Specific filaggrin mutations cause ichthyosis vulgaris and are significantly associated with atopic dermatitis in Japan. *J Invest Dermatol* 128:1436–41

Nomura T, Sandilands A, Akiyama M *et al.* (2007) Unique mutations in the filaggrin gene in Japanese patients with ichthyosis vulgaris and atopic dermatitis. *J Allergy Clin Immunol* 119:434–40

Rodríguez E, Baurecht H, Herberich E *et al.* (2009) Meta-analysis of filaggrin polymorphisms in eczema and asthma: robust risk factors in atopic disease. *J Allergy Clin Immunol* 123:1361–70

Sandilands A, Terron-Kwiatkowski A, Hull PR *et al.* (2007) Comprehensive analysis of the gene encoding filaggrin uncovers prevalent and rare mutations in ichthyosis vulgaris and atopic eczema. *Nat Genet* 39:650–4

van den Oord RA, Sheikh A (2010) Filaggrin gene defects and risk of developing allergic sensitisation and allergic disorders: systematic review and meta-analysis. *BMJ* 339:b2433

See related commentary on pg 2703

RNase 7 Protects Healthy Skin from *Staphylococcus aureus* Colonization

Journal of Investigative Dermatology (2010) **130,** 2836–2838; doi:10.1038/jid.2010.217; published online 29 July 2010

TO THE EDITOR

The Gram-positive bacterium *Staphylococcus aureus* is an important pathogen that causes various skin infections (Miller and Kaplan, 2009). However, healthy skin is usually not infected by *S. aureus,* despite the high carrier rates in the normal population (Noble, 1998). This suggests that the cutaneous defense system has the capacity to effectively control the growth of *S. aureus.* There is increasing evidence that antimicrobial proteins are important effectors of the cutaneous defense system (Harder *et al.*, 2007). A recent study reported that keratinocytes contribute to cutaneous innate defense against *S. aureus* through the production of human β-defensin-3 (Kisich *et al.*, 2007). In addition to human β-defensin-3,, other antimicrobial proteins may also participate in cutaneous defense against *S. aureus.* One candidate is RNase 7, a potent antimicrobial ribonuclease that is highly expressed in healthy skin (Harder and Schröder, 2002; Köten *et al.*, 2009).

To investigate the hypothesis that RNase 7 may contribute to protect healthy skin from *S. aureus* colonization, we first incubated natural RNase 7 isolated from stratum corneum skin extracts (Harder and Schröder, 2002) with *S. aureus* (ATCC 6538). In concordance with our initial report about RNase 7 (Harder and Schröder, 2002), we verified that RNase 7 exhibited a high killing activity against *S. aureus* (lethal dose of 90% = 3–6 μg ml^{-1}).

Recently, we reported a moderate induction of RNase 7 mRNA expression in primary keratinocytes treated with heat-killed *S. aureus* (Harder and Schröder, 2002). To assess the induction of RNase 7 by *S. aureus* in the

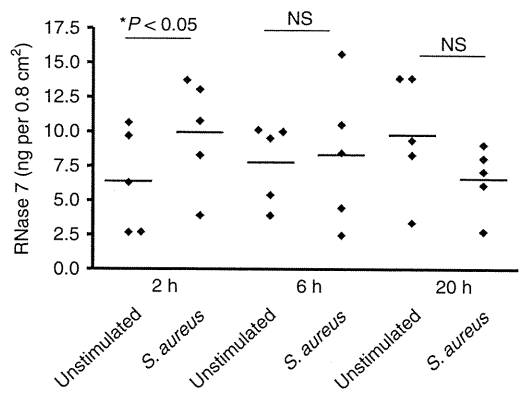

Figure 1. Induced secretion of RNase 7 on the skin surface on treatment with living *S. aureus*. Defined areas (0.8 cm^2) of skin explants derived from plastic surgery were incubated with or without approximately 1,000 colony-forming units of *S. aureus* (ATCC 6538) in 100 μl of sodium phosphate buffer. After 2, 6, and 20 hours, the concentration of secreted RNase 7 was determined by ELISA. Stimulation with *S. aureus* for 2 hours revealed a significant induction as compared with the unstimulated control after 2 hours (*P<0.05, Student's *t*-test; n.s. = not significant). Data shown are means of triplicates of five skin explants derived from five donors.

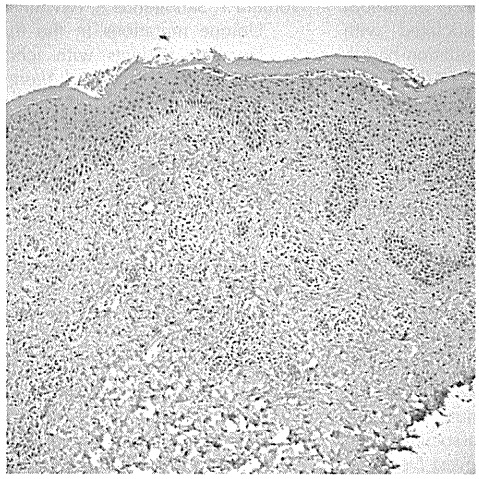

Fig 2. Immunohistochemistry of skin for angiopoietin-2. Note the abundant staining in the basal epidermis and dermal inflammatory cells. (Original magnification: ×100.)

National Institutes of Health, and a Veterans Administration Hospital Merit Award (to J.L.A.)

Conflicts of interest: None declared.

Reprint requests: Jack L. Arbiser, MD, PhD, Department of Dermatology, Emory University School of Medicine, WMB 5309, 1639 Pierce Dr, Atlanta, GA 30322.

E-mail: jarbise@emory.edu

REFERENCES

1. Bhandarkar SS, MacKelfresh J, Fried L, Arbiser JL. Targeted therapy of oral hairy leukoplakia with gentian violet. J Am Acad Dermatol 2008;58:711-2.
2. Lambeth JD, Kawahara T, Diebold B. Regulation of Nox and Duox enzymatic activity and expression. Free Radic Biol Med 2007;43:319-31.
3. Perry BN, Govindarajan B, Bhandarkar SS, Knaus UG, Valo M, Sturk C, et al. Pharmacologic blockade of angiopoietin-2 is efficacious against model hemangiomas in mice. J Invest Dermatol 2006;126:2316-22.
4. Brockow K, Grabenhorst P, Abeck D, Traupe B, Ring J, Hoppe U, et al. Effect of gentian violet, corticosteroid and tar preparations in *Staphylococcus aureus*–colonized atopic eczema. Dermatology 1999;199:231-6.
5. Howell MD, Novak N, Bieber T, Pastore S, Girolomoni G, Boguniewicz M, et al. Interleukin-10 downregulates anti-microbial peptide expression in atopic dermatitis. J Invest Dermatol 2005;125:738-45.

doi:10.1016/j.jaad.2009.05.027

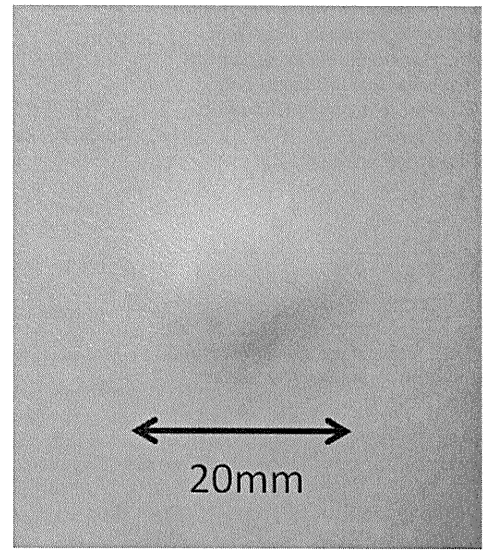

Fig 1. A slightly violaceous nodule on the middle aspect of the left thigh.

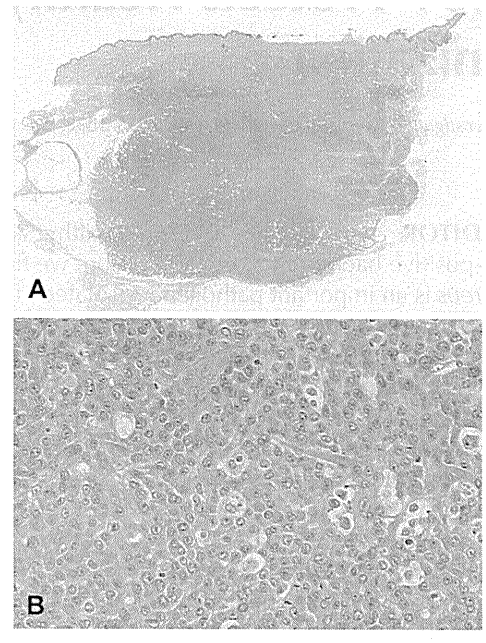

Fig 2. Skin biopsy findings. **A**, Dense, nodular, diffuse infiltrate of monotonous uniform cells involving the dermis and subcutaneous fat. **B**, A nodule of cells with round nuclei; prominent single or multiple nucleoli; abundant pale, slightly eosinophilic cytoplasm; and a number of atypical mitotic figures.

Aleukemic leukemia cutis with extensive bone involvement

To the Editor: Aleukemic leukemia cutis (ALC) is a rare condition that is characterized by the invasion of leukemic cells into the skin before such cells are observed in the peripheral blood.[1] We present a case of ALC with multiple bone metastases.

An 81-year-old man had a 2-month history of asymptomatic nodules on his trunk and legs. The physical examination revealed five subcutaneous nodules measuring up to 10 mm in size on his back and legs and a firm, slightly violaceous nodule

Fig 3. A positron emission tomography scan reveals extensive high-density areas in the bone and in the subcutaneous tissue of the trunk and the extremities, suggesting multiple metastases.

measuring 20 mm in diameter on the middle aspect of his left thigh (Fig 1). A complete blood cell count and chemical analysis showed no pathologic changes. Histopathologic examination of a skin biopsy specimen revealed a dense, nodular, diffuse infiltrate of monotonous uniform cells with round nuclei, prominent single or multiple nucleoli, and abundant pale, slightly eosinophilic cytoplasmic cells throughout the dermis and subcutaneous fat (Fig 2, *A*). A number of atypical mitotic figures were seen (Fig 2, *B*). The tumor cells were positive for leukocyte common antigen, CD68, and myeloperoxidase. A histologic diagnosis of myeloid leukemia cutis with possible monocytic lineage was made. However, bone marrow aspiration showed neither an increase in blasts nor abnormal cell infiltration, and repeated peripheral blood cell counts were normal, with no atypical cells. A diagnosis of ALC was established. Positron emission tomography (PET) revealed extensive high-density areas in the bone and subcutaneous tissue, suggesting multiple metastases (Fig 3). Seven weeks after his first visit, a peripheral blood cell examination disclosed 8% atypical monocytic cells, suggesting a diagnosis of acute myeloid leukemia. The patient refused other studies and died 1 week later.

ALC is a rare form of leukemia with a poor prognosis. The term "aleukemic" has been used to designate a form of leukemia in which there are no leukemic cells in the blood.[2] ALC precedes peripheral blood or bone marrow abnormalities at least 1 month before the systemic findings. Once leukemic cells appear in the peripheral blood or bone marrow, the mean survival time ranges from 3 to 30 months.[3,4] The clinical features of ALC include multiple papules, nodules, or infiltrated plaques with a red-brown or plum-colored surface. Histologic findings show the infiltration of leukemic cells in the dermal or subcutaneous tissues. The cytologic features of the tumor cells include large, vesicular nuclei and multiple prominent nucleoli.[3] Because of the rarity of the disease, there is no consensus on the treatment of choice for ALC; radiotherapy, chemotherapy, and total body electron therapy have achieved variable results.[1,3-8] A study by Chang et al[4] of a large group of ALC patients showed that the most common extramedullary site of involvement after the skin (31 of 31 patients) was the lymph nodes (8 of 31 patients) followed by the spleen (2 of 31 patients). Although no reports of a clinical presentation of ALC with multiple sites of bone infiltration were found in a thorough search of the English-language literature, extramedullary leukemia is known to occur in bone.[5] We emphasize that the routine assessment of a patient with ALC should include systemic investigations such as PET, taking into consideration the possibility of bone involvement.

Maria Maroto Iitani, MD, MSc,[a] Riichiro Abe, MD, PhD,[a] Teruki Yanagi, MD,[a] Asuka Hamasaka, MD, PhD,[a] Yasuki Tateishi, MD, PhD,[a] Yukiko Abe, MD, PhD,[a] Miki Ito, MD,[b] Takeshi Kondo, MD, PhD,[c] Kanako Kubota, MD, PhD,[d] and Hiroshi Shimizu, MD, PhD[a]

Departments of Dermatology, Hokkaido University Graduate School of Medicine[a] and the National Hospital Organization Hokkaido Cancer Center[b]; Departments of Gastroenterology and Hematology,[c] Hokkaido University Graduate School of Medicine; and the Department of Surgical Pathology,[d] Hokkaido University Hospital, Sapporo, Japan

Funding sources: None.

Conflicts of interest: None declared.

Reprint requests: Maria Maroto Iitani, MD, MSc, Department of Dermatology, Hokkaido University Graduate School of Medicine, North 15, West 7, Kita-ku, Sapporo 060-8638, Japan.

E-mail: miitani@med.hokudai.ac.jp

REFERENCES

1. Ohno S, Yokoo T, Ohta M, Yamamoto M, Danno K, Hamato N, et al. Aleukemic leukemia cutis. J Am Acad Dermatol 1990;22 (2 pt 2):374-7.
2. Yoder FW, Shuen RL. Aleukemic leukemia cutis. Arch Dermatol 1976;112:367-9.
3. Okun MM, Fitzgibbon J, Nahass GT, Forsman K. Aleukemic leukemia cutis, myeloid subtype. Eur J Dermatol 1995;5:290-3.
4. Chang H, Shih LY, Kuo TT. Primary aleukemic myeloid leukemia cutis treated successfully with combination chemotherapy: report of a case and review of the literature. Ann Hematol 2003;82:435-9.
5. Lee B, Fatterpekar GM, Kim W, Som PM. Granulocytic sarcoma of the temporal bone. AJNR Am J Neuroradiol 2002;23:1497-9.
6. Török L, Lueff S, Garay G, Tápai M. Monocytic aleukemic leukemia cutis. J Eur Acad Dermatol Venerol 1999;13:54-8.
7. Tomasini C, Quaglino P, Novelli M, Fierro MT. "Aleukemic" granulomatous leukemia cutis. Am J Dermatopathol 1998;20:417-21.
8. Imanaka K, Fujiwara K, Satoh K, Kuroda Y, Takahashi M, Sadatoh N, et al. A case of aleukemic monocytic leukemia cutis treated with total body electron therapy. Radiat Med 1988;6:229-31.

doi:10.1016/j.jaad.2009.05.040

Onychopapilloma presenting as longitudinal leukonychia

To the Editor: Onychopapilloma is an uncommon benign nail neoplasm characterized histologically by distal subungal hyperkeratosis and nail matrix metaplasia of the nail bed with marked papillomatosis. The majority of cases present clinically as localized longitudinal erythronychia. We report a case of onychopapilloma presenting as localized longitudinal leukonychia.

A 50-year-old woman was referred for the evaluation of dystrophy of the right third fingernail. The nail plate had split distally for several years. Her medical history was noncontributory. The physical examination revealed a 1-mm wide band of longitudinal leukonychia with a slight longitudinal ridge on the right third fingernail. No erythronychia was present. Distally, there was a V-shaped notch and split, with a keratotic 1-mm papule at the hyponychium (Fig 1). The other nails were normal. Lateral nail plate curl avulsion exposed a longitudinal ridge extending from the midmatrix onto the nail bed. A longitudinal biopsy from matrix to hyponychium was performed. On histologic examination, the nail bed exhibited slender, elongated, and hyperplastic rete ridges with underlying fibrosis and thickening of the fibrovascular dermal stroma. Upper nail bed keratinocytes were large and exhibited ample pink cytoplasm similar to the nail matrix keratogenous zone. Hyperkeratosis was seen at the hyponychium (Fig 2). A periodic acid–Schiff test did not reveal fungal elements. These findings were consistent with the diagnosis of onychopapilloma.

Fig 1. Fingernail with a 1-mm wide band of longitudinal leukonychia and distal V-shaped splitting, onycholysis, and a keratotic papule at the free edge of the nail. Dermatoscopy highlights these findings (*inset*).

Onychopapilloma was first reported in 1995 by Baran and Perrin,[1] who described four cases of "distal subungual keratosis with multinucleate cells." The term "onychopapilloma" was later coined in 2000 when the authors reported a second series of 14 cases with similar clinical and histopathologic features.[2] Key among these features were the upper cell layers in the nail bed epithelium exhibiting abundant eosinophilic cytoplasm resembling the nail matrix keratogenous zone, and was thought to indicate matrix metaplasia of the nail bed epithelium. Additional findings included acanthosis and papillomatosis of the distal nail bed epithelium. Multinucleated cells were found variably. In both series, all lesions presented as either longitudinal erythronychia or longitudinal bands of splinter hemorrhages, several of which were associated with distal onycholysis. Other occurrences of suspected onychopapilloma have been reported, including one case representing solitary nail bed lichen planus, and also in the spectrum of localized longitudinal erythronychia.[3] In addition to onychopapilloma, the differential diagnosis for localized longitudinal erythronychia includes Bowen disease,[2,3] and histologic investigation is often warranted.

Journal of Surgical Research **163,** e23–e34 (2010)
doi:10.1016/j.jss.2010.04.044

Donor Pretreatment with DHMEQ Improves Islet Transplantation

Tohru Takahashi, M.D.,*,[1] Shuichiro Matsumoto, M.D., Ph.D.,* Michiaki Matsushita, M.D., Ph.D.,* Hirofumi Kamachi, M.D., Ph.D.,* Yosuke Tsuruga, M.D., Ph.D.,* Hironori Kasai, M.D.,* Masaaki Watanabe, M.D.,* Michitaka Ozaki, M.D.,† Hiroyuki Furukawa, M.D., Ph.D.,* Kazuo Umezawa, Ph.D.,‡ and Satoru Todo, M.D., Ph.D.*

**Department of General Surgery, Hokkaido University Graduate School of Medicine, Sapporo, Hokkaido, Japan; †Department of Molecular Surgery, Hokkaido University Graduate School of Medicine, Sapporo, Hokkaido, Japan; and ‡Department of Applied Chemistry, Faculty of Science and Technology, Keio University, Yokohama, Kanagawa, Japan*

Submitted for publication December 19, 2009

Background. **Currently, pancreatic islet transplantation to achieve normoglycemia in insulin-dependent diabetes mellitus (IDDM) requires two or more donors. This may be due to the inability to transplant functionally preserved and viable islets after isolation. Islets have already been subjected to various harmful stresses during the isolation process leading to apoptosis. One of the intracellular signaling pathways, the transcription factor nuclear factor-κB (NF-κB)-related pathway, is relevant to the mechanism of β-cell apoptosis in isolated islets. We attempted to prevent islet apoptosis during isolation by a novel NF-κB inhibitor, dehydroxymethylepoxyquinomicin (DHMEQ).**

Materials and Methods. **DHMEQ was injected intraperitoneally into donor mice 2 h prior to isolation. NF-κB activation, the functioning of isolated islets, apoptosis after isolation, and cytokine- and apoptosis-related genes were analyzed. After 160 equivalents of islets were transplanted into diabetic mice, graft survival and function were evaluated.**

Results. **Intra-islet NF-κB was activated immediately after isolation, and DHMEQ inhibited NF-κB activation without deterioration of islet function. DHMEQ significantly prevented apoptosis by inhibiting caspase 3/7 activities and down-regulated Bax, a pro-apoptotic gene. Donor pretreatment with DHMEQ significantly improved engraftment in syngeneic islet transplantation in mice, thus preserving insulin contents in the graft liver, as assessed by functional and histologic analyses.**

Conclusions. **DHMEQ is a promising agent in islet transplantation because it protects islets from apoptosis during isolation stress. Donor pretreatment with DHMEQ can significantly affect the success of islet engraftment.**

Key Words: **islet transplantation; donor pretreatment; DHMEQ; NF-κB inhibitor; NF-κB; islet isolation; apoptosis; mouse.**

INTRODUCTION

Islet transplantation for insulin-dependent diabetes mellitus (IDDM) by the Edmonton protocol has been highly successful, but this therapeutic approach has a major limitation in that islets from two to four cadaveric pancreases are required to achieve insulin independence in one diabetic recipient [1]. Recently, the reported success of human islet transplantation has further emphasized the imbalance between the supply and demand of islet tissues for transplantation [2]. The viability of islets is lost in the course of procurement to transplantation [3]. Therefore, the prevention of islet loss is important for improving engraftment and for reducing the number of islets required to achieve normoglycemia in diabetes. This, in turn, will allow us to optimize the number of transplants that can be performed given the current limited supply of islets. To define strategies to preserve the transplanted β-cell mass, it is essential to know the extent of β-cell loss and to identify the mechanisms underlying β-cell destruction and protection.

Islets have already been susceptible to various harmful stresses, such as ischemia, disruption from the extracellular matrix due to preservation, digestion,

[1] To whom correspondence and reprint requests should be addressed at Department of General Surgery, Hokkaido University Graduate School of Medicine, North 14 West 5, Kitaku, Sapporo, Hokkaido 060-8648, Japan. E-mail: Ttohru616@aol.com.

0022-4804/$36.00

isolation, and culture. These procedures are thus expected to lead islets to apoptosis, which would be the major cause of islet loss [3, 4]. Although the mechanism underlying β-cell apoptosis after isolation is not clearly understood, the transcription factor nuclear factor-κB (NF-κB) [5, 6] is considered to be involved in β-cell apoptosis.

NF-κB is a family of inducible transcription regulatory proteins expressed in a variety of tissues [7]. Some studies have reported that NF-κB was upregulated in isolated islets and that cytokines such as IL-1β, IFNγ, and TNFα were produced from them by NF-κB activation. Then, intra-islet cytokine production [8] can further aggravate the apoptotic pathway. On the other hand, NF-κB also regulates pro- [9, 10] or anti-apoptotic genes [11]. Hence whether NF-κB has an inducible or inhibitory effect on apoptosis is a matter of controversy. However, many recent studies have verified that NF-κB inhibition protects insulin-secreting cell lines or primary islets from cytokine-induced apoptosis [6, 12, 13].

A novel NF-κB inhibitor, dehydroxymethylepoxyquinomicin (DHMEQ), is a 5-dehydroxymethyl derivative of epoxyquinomicin C, an antibiotic originally isolated from *Amycolatopsis* sp [14] that has been found to inhibit NF-κB activation at the level of nuclear translocation [15]. DHMEQ can abrogate constitutive NF-κB activity and inhibit the production of proinflammatory cytokines from various cells [16, 17]. These findings suggest that DHMEQ may be a new therapeutic agent for inflammatory diseases.

In the current study, we attempted to inhibit intraislet NF-κB activation during isolation by DHMEQ. We aimed to prevent islet apoptosis by inhibiting inflammatory cytokines or by regulating apoptosis-related genes and to preserve the islet's ability to release insulin.

MATERIALS AND METHODS

Animals

Male C57BL/6J mice, aged 9–12 wk, were purchased from Clea Japan, Inc. (Tokyo, Japan) and used as donors and recipients. All studies were performed in accordance with the Guide for the Care and Use of Laboratory Animals at Hokkaido University Graduate School of Medicine.

Islet Isolation and Culture

DHMEQ, dissolved in 2.4% dimethyl sulfoxide (DMSO) (Sigma, St. Louis, MO) and 0.5% carboxymethylcellulose (CMC) (Sigma) or vehicle (DMSO with CMC) was given by intraperitoneal injection (i.p.) to donors 2 h before isolation. DHMEQ was administered at 12 mg/kg. Pancreatic islets were distended by intraductal injection of collagenase (2 mg/mL; Worthington Biochemical, Lakewood, NJ), and digestion was performed at 37°C for 20 min. The islets were separated on Ficoll (Sigma) density gradients by centrifugation at 2200 rpm for 10 min, and the isolated islets were counted under a scaled microscope at 40× to calculate islet equivalents (IEQ). One IEQ was the islet tissue mass equivalent to a spherical islet 150 μm in diameter. Islets were hand-picked individually under the microscope to ensure pure islet preparations. The islets were cultured in RPMI-1640 (Sigma) medium supplemented with 10% FCS (Gibco, Long Island, NY) and antibiotic antimycotic solution (100 units/mL penicillin, 0.1 mg streptomycin, and 0.25 μg amphotericin B) (Sigma) in a 5% CO_2 humidified atmosphere at 37°C.

Analysis of NF-κB Transcriptional Activity

Islets treated with vehicle or DHMEQ were isolated, and nuclear proteins were extracted 30 min after isolation by using NE-PER nuclear and cytoplasmic extraction reagents (Pierce Chemical Co., Rockford, IL) according to the manufacturer's instructions. Protein concentrations were determined by the BCA Protein Assay Reagent Kit (Pierce Chemical Co.). NF-κB DNA-binding activity in the nuclear extract (NE) was measured using the Trans-AM NF-κB p65 enzyme-linked immunosorbent assay (ELISA) kit (Active Motif Japan, Tokyo, Japan) according to the manufacturer's instructions. Briefly, 1.5 μg NE was added to a 96-well plate, to which an oligonucleotide-containing NF-κB consensus-binding site had been immobilized. The NF-κB complex bound to the oligonucleotide was detected by adding a specific monoclonal antibody (mAb) to a p65 subunit. A secondary horseradish peroxidase (HRP)-conjugated mAb was added and developed with a tetramethylbenzidine substrate. After an optimal development time, the reaction was stopped using H_2SO_4 0.5 mol/L, and absorbance was measured by 450 nm. The specificity of the assay was monitored by competition experiments using NF-κB wild-type and mutant consensus oligonucleotides provided in the kit. The activated form of NF-κB exists only in the nuclear fraction, and this kit detects only this activated form. NF-κB activation in three different nuclear extracts ($n = 3$) was checked by comparison with the NF-κB level of cytosol protein, positive control (PC), and negative control (NC) provided in the kit, which were simultaneously measured.

Static Glucose-Stimulated Insulin Secretion (GSIS)

After islets were cultured at 37°C for 12 or 24 h, 20 islets were hand-picked and incubated for 60 min in RPMI-1640 with 10% FCS containing 1.67 mM glucose. Thereafter, the solution was changed and the islets were incubated for 60 min with 0.5 mL of 1.67 mM glucose, then 16.7 mM glucose in RPMI-1640 with 10% FCS at 37°C. Supernatants were collected for baseline and stimulated insulin release, and were stored at −20°C. Subsequently, the insulin contents of the supernatants ($n = 6$) were analyzed using ELISA (Shibayagi, Gunma, Japan). A stimulation index was calculated by dividing the total insulin amount released from islets cultured in the high-glucose medium by the total insulin amount released from islets cultured in the low-glucose medium.

Real-Time PCR for Cytokine- and Apoptosis-Related Gene Expression in Isolated Islets

Total RNA was isolated from mouse primary islets using the Qiagen RNeasy kit (Qiagen, Valencia, CA). cDNA was reverse-transcribed using Omniscript (Qiagen) for 60 min at 37°C. Amplification of resultant cDNA was performed by PCR with TAKARA Ex Taq (Takara Bio, Ohtsu, Japan). To measure murine monocyte chemoattractant protein-1 (MCP-1), IL-1β, Bax, Bcl-2, and β-actin expression, real-time PCR was performed using an ABI-Prism 7000 sequence detector (Applied Biosystems, Foster City, CA). The PCR reaction was performed in a 25 μL reaction volume that contained 1 μL (100 ng) of the template cDNA, 200 nM each of the sense and antisense primers, and 2× Power SYBR Green PCR Master Mix (Applied Biosystems) in duplicate. PCR amplification profiles included an initial incubation at 50°C for 2 min, denaturation at 95°C for 5 min, and 40 cycles at 95°C for 30 s and 60°C for 1 min. Primer sequences (Invitrogen, Carlsbad,

TABLE 1

Primer Sequences of Real-Time PCR and Product Size

Gene	Sequences	Size (bp)
MCP-1	forward 5′-ACCTGCTGCTACTCATTCACC-3′ reverse 5′-CATTCCTTCTTGGGGTCAG-3′	149
IL-1β	forward 5′-AGTTGACGGACCCCAAAAG-3′ reverse 5′-GTGATACTGCCTGCCTGAAG-3′	125
Bax	forward 5′-TGGAGATGAACTGGACAGCA-3′ reverse 5′-GAAGTTGCCATCAGCAAACA-3′	118
Bcl-2	forward 5′-AGTACCTGAACCGGCATCTG-3′ reverse 5′-CATGCTGGGGCCATATAGTT-3′	82
β-actin	forward 5′-CTGTATTCCCCTCCATCGTG-3′ reverse 5′-AATGGGGTACTTCAGGGTCA-3′	128

CA) and the sizes of the fragments generated by PCR reactions are shown in Table 1.

The relative standard curve method was used to quantify mRNA levels against a murine cell line, RAW264.7. A standard curve was developed based on the principle that a plot of the log of the diluted cDNA contents of the standard *versus* the threshold cycle results in a straight line. The level of sample mRNA was normalized for β-actin as an internal control.

Terminal Deoxynucleotidyl Transferase-Mediated Deoxyuridine Triphosphate Nick End Labeling (TUNEL) Assay

Donor-pretreated islets with or without DHMEQ were incubated for 48 h and fixed overnight in a solution of 4% formaldehyde (Sigma). The islets were embedded in paraffin, and 5 μm sections were deparaffinized, rehydrated, and incubated with proteinase K at room temperature for 15 min. They were then stained by the TUNEL method using the *in situ* Apoptosis Detection Kit (Takara Bio). The final reaction product was visualized by 3,3′-diaminobenzidinetetrahydrochloride (Sigma). To calculate an apoptotic index, the number of cells positive for the TUNEL reaction was determined and expressed as a percentage of the total number of cells counted. Sections were prepared from three different isolations in each group. Five fields, each containing at least 600 cells, were analyzed at 200× magnification per section, and 15 islets of 150 μm mean diameter for each counting were evaluated.

Caspase 3/7 Activity

Isolated islets were cultured in a 35 mm dish for floating cells containing RPMI-1640 medium. The islets were cultured for 24 or 48 h at 37°C, 5% CO_2. After incubation, 100 islets were hand-picked and transferred to a 1.5 mL Eppendorf tube. The tubes were centrifuged, and the islets were resuspended in 100 μL of RPMI-1640. Caspase-3 activity was measured using the Caspase-Glo 3/7 Assay (Promega Corp., Madison, WI) according to the manufacturer's instructions. Islets were lysed using the Caspase-Glo 3/7 reagent and incubated at room temperature for 1 h. Luciferase activity was measured using a GloMax 20/20 n luminometer (Promega) ($n = 6$).

Islet Transplantation

Male C57BL/6J mice were rendered diabetic by an i.p. of 180 mg/kg streptozotocin (STZ) (Sigma) freshly dissolved in citrate buffer (pH 4.5) and transplanted 7 d after STZ administration. Diabetes was considered to be present when nonfasting blood glucose levels were >450 mg/dL in two consecutive measurements. DHMEQ was given i.p. into donors 2 h prior to isolation of pancreatic islets. For each animal, 160 IEQs were transplanted *via* the portal vein; control ($n = 16$), DHMEQ ($n = 12$). Blood glucose levels were measured to evaluate graft function during the 60-day post-transplantation period. Normoglycemia was considered to be present when blood glucose levels were <200 mg/dL for two consecutive days.

Intraperitoneal Glucose Tolerance Test (IPGTT)

IPGTT was performed in transplanted mice (control: $n = 12$, DHMEQ: $n = 12$) with pretreated donor islets on postoperative day 28, and nontransplanted age-matched C57BL/6J mice ($n = 8$) served as controls. The mice were fasted for 6 h and given i.p. with 20% glucose at a dose of 2 g/kg BW. The animals were then monitored for blood glucose levels at 0, 30, 60, 90, 120, and 180 min after the injection. The area under the curve (AUC) for the IPGTT was evaluated. During the IPGTT, care was taken not to cause any unnecessary stress in the animals, and they had free access to water.

Insulin Content of Islet-Transplanted Graft Liver

The whole liver was extracted, suspended in 2 mL of distilled water, sonicated for 30 s, and added to more distilled water to a total of 3 mL, then resuspended in 7 mL of acid/ethanol (0.18 mol/L HCl in 99.5% ethanol). Insulin was extracted overnight at 4°C. Tubes were centrifuged at 3000 rpm for 10 min at 4°C, and the supernatant was stored at –20°C for future insulin determination. After neutralization, the insulin content in the extracts was measured by ELISA (control: $n = 13$, DHMEQ: $n = 11$).

Histological Analyses of Islet-Transplanted Graft Liver

Graft livers were removed 24 h after islet transplantation, fixed in 4% formalin for 24 h, and embedded in paraffin for hematoxylin-eosin (HE) and TUNEL staining. Serial-matched paraffin sections were used for these stainings. The sections were then immunostained for insulin using a guinea pig polyclonal anti-insulin primary antibody (DAKO, Glostrup, Denmark) and alkaline phosphatase-conjugated AffiniPure donkey anti-guinea pig IgG secondary antibody (Jackson Immuno-Research, West Grove, PA). The area of islet necrosis assessed by HE sections was measured by Image J software (NIH, Bethesda, MD) and was expressed as a percentage of whole islet tissue. Three mice were transplanted for each group as three independent experiments, and 8.6 islets per graft at the mean number were assessed.

Statistical Analysis

Results are presented as means ± standard deviation (SD). Statistical analyses were performed using Student's t-test and the Mann-Whitney t-test where appropriate. Differences in the duration of graft survival between groups were evaluated with the Kaplan-Meier log-rank test. A P value < 0.05 was considered statistically significant.

RESULTS

Assessment of Molecular and Morphologic Changes in Islet During Isolation Procedure—

NF-κB Activation and Effect of DHMEQ During Isolation Procedure

The level of NF-κB in NE in either group was higher than that of cytosol protein, and that of cytosol protein was nearly the same as that of NC. This means intraislet NF-κB was activated immediately after isolation. The level of NF-κB in the DHMEQ-treated group was

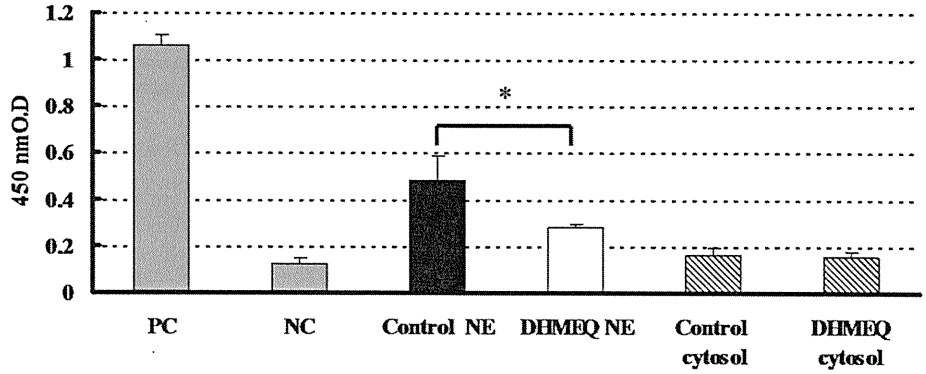

FIG. 1. NF-κB (p65) activation levels immediately after isolation. All data are representative of three independent experiments and are expressed as means ± standard deviation (SD) ($n = 3$). PC = positive control; NC = negative control; NE = nuclear extract. Intraislet NF-κB was activated immediately after isolation, and the level of NF-κB in the DHMEQ-treated group was significantly lower than that of the control. *$P < 0.05$ *versus* control.

significantly lower than that of the control ($P < 0.05$) (Fig. 1). DHMEQ significantly inhibited NF-κB activation in the isolated islets.

GSIS

The responses to low glucose are almost the same and did not decline during culture in either group. The responses to high glucose were almost the same, but declined slightly during culture in both groups (Fig. 2A). So, the stimulation indices of both groups showed a rapid drop during culture (Fig. 2B). The reduction rates of stimulation indices in the control and DHMEQ-treated groups from 12 to 24 h were 47.8% and 25.0%, respectively. Although stimulation indices of the DHMEQ-treated group look well preserved during culture, there was no significant difference among groups.

Cytokine Expression in Isolated Islets

The MCP-1 mRNA expression levels of the DHMEQ-treated group at 6 h were slightly lower than those of the control, but no significant differences were observed (Fig. 3A). The IL-1β mRNA levels of the control and DHMEQ-treated groups were 0.079 ± 0.011 and

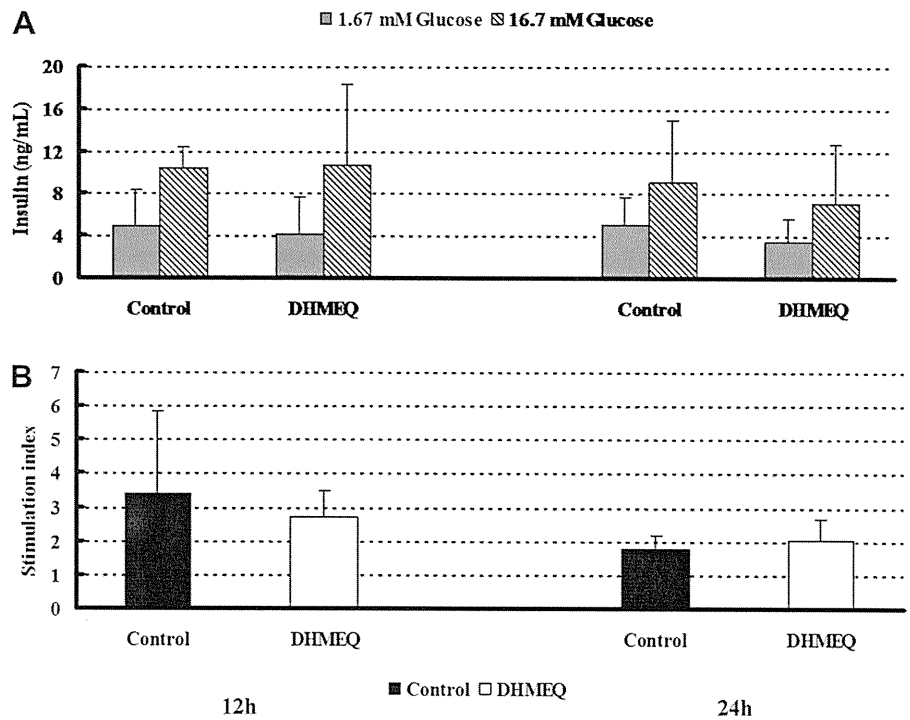

FIG. 2. GSIS. The raw data (A) and a stimulation index (B) are representative of six independent experiments, and are expressed as means ± SD ($n = 6$). There was no significant difference between the control and DHMEQ-treated groups.

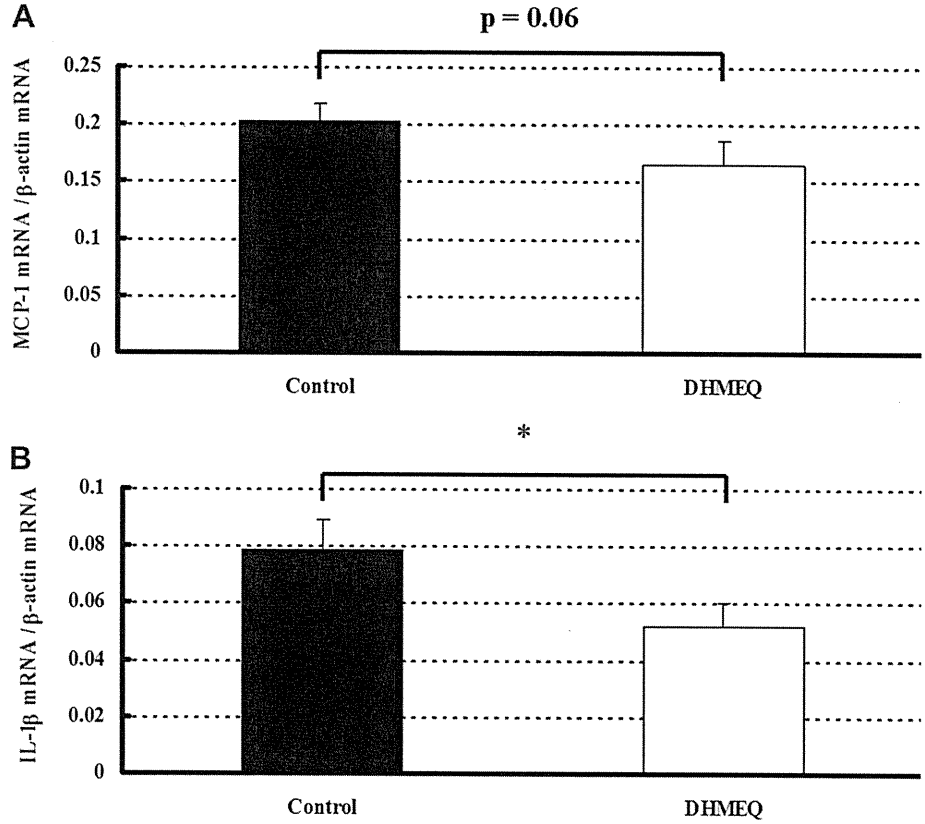

FIG. 3. Cytokine expression in isolated islets. (A) The MCP-1 expression in the DHMEQ-treated group at 6 h after isolation was lower than that of the control group, but significant differences were not observed ($P = 0.06$). (B) The IL-1β expression in the DHMEQ-treated group at 6 h after isolation was significantly lower than that of the control. Results are representative of three independent experiments and are expressed as means ± SD ($n = 3$). *$P < 0.05$ *versus* control.

0.052 ± 0.008 at 6 h, respectively, and those of the DHMEQ-treated group were significantly inhibited compared to those of the control ($P < 0.05$) (Fig. 3B).

Bax and Bcl-2 Expression in Isolated Islets

The Bax expression of the DHMEQ-treated group (2.27 ± 0.27) was significantly lower than that of the control (2.88 ± 0.24) at 6 h after isolation ($P < 0.05$) (Fig. 4A). There were no significant differences in Bcl-2 expression between the groups. DHMEQ did not inhibit Bcl-2 expression (Fig. 4B).

TUNEL Assay

The apoptotic indices of the DHMEQ-treated group (2.97% ± 2.59%) were significantly lower than those of the control (8.12% ± 5.18%) at 48 h after isolation ($P < 0.01$) (Fig. 5A). The representative islets of the control (Fig. 5B) and DHMEQ-treated groups (Fig. 5C) were displayed.

Caspase 3/7 Activity

The caspase 3/7 activities of control after isolation were gradually up-regulated, but those of the DHMEQ-treated group were constant. The activities of the DHMEQ-treated group at 24 h (1,265,812 ± 158,922 RLU) ($P < 0.05$) and 48 h after isolation (1,162,761 ± 242,885 RLU) ($P < 0.01$) were significantly lower than those of the control (1,565,278 ± 354,297 RLU at 24 h and 1,998,846 ± 378,921 RLU at 48 h, respectively) (Fig. 6).

Effect of DHMEQ Treatment on Donor After Syngeneic Intraportal Islet Transplantation

Islet Graft Survival

The blood glucose levels of the control were almost always high during the first 60 post-operative d, but in a few mice, blood glucose levels did not decrease until 4 wk after transplantation and reached normoglycemia thereafter ($n = 16$) (Fig. 7A). However, almost all mice in the DHMEQ-treated group (Fig. 7B) reached normoglycemia earlier than 14 days after transplantation ($n = 12$). The reversal rates of hyperglycemia at 60 days in the DHMEQ-treated group (83.3%) were significantly higher than those in the control group (31.2%) ($P < 0.01$) (Fig. 7C).

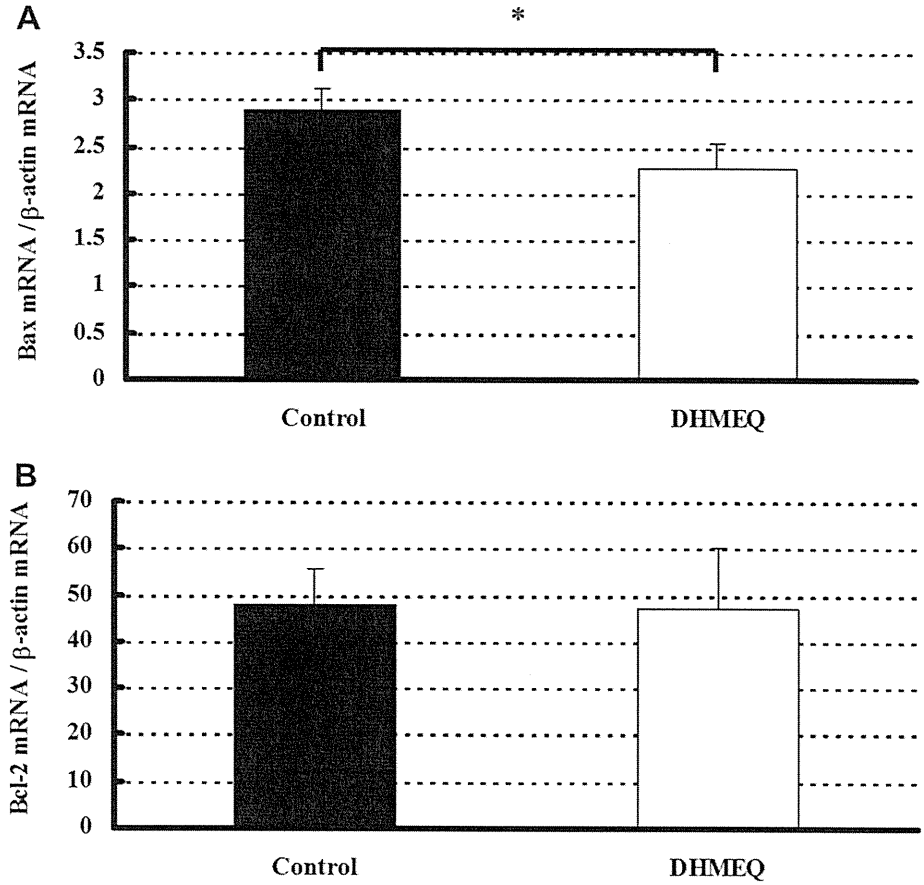

FIG. 4. Apoptosis-related gene expression in isolated islets. (A) Bax expression in the DHMEQ-treated group at 6 h after isolation was significantly lower than that of the control. (B) Bcl-2 expression in the isolated islets. No significant differences were observed between the groups. Results are representative of three independent experiments and are expressed as means ± SD ($n = 3$). *$P < 0.05$ *versus* control.

IPGTT

The time courses of blood glucose levels after intraperitoneal glucose loading in the DHMEQ-treated group were similar to those of normal mice, but the DHMEQ groups responded less than the normal mice did. The control group barely responded to glucose loading, and blood glucose levels were higher than those of the DHMEQ-treated group throughout the experiment. The blood glucose levels of the DHMEQ-treated group at 120 min (349.4 ± 96.0 mg/dL) and 180 min (234.8 ± 106.1 mg/dL) were significantly lower than those of the control group (462.0 ± 99.7 mg/dL) ($P < 0.05$), (415.9 ± 148.7 mg/dL) ($P < 0.01$), respectively (Fig. 8A). The AUCs for IPGTT of the DHMEQ-treated group (1161.5 ± 240.5) were significantly lower than those of the control (1422.7 ± 266.3) ($P < 0.05$) (Fig. 8B).

Insulin Content of Islet-Transplanted Graft Liver

Insulin contents per graft in the control and DHMEQ-treated groups were 1194.49 ± 1206.93 ng/graft and 2485.05 ± 1481.06 ng/graft, respectively. The insulin contents of the DHMEQ-treated group were significantly higher than those of the control group ($P < 0.05$) (Table 2).

Histological Analyses of Islet-Transplanted Graft Liver

The necrotic areas in the DHMEQ-treated group (26.2% ± 26.8%) (Fig. 9B) were significantly smaller than those of the control group (77.6% ± 28.7%) ($P < 0.01$) (Fig. 9A). Insulin secretory granules with many apoptotic cells were noted in the control group (Fig. 9C), but the islets of the DHMEQ-treated group had distinguished features with well-preserved nuclei, numerous secretory granules, and no apoptotic cells (Fig. 9D).

DISCUSSION

Islets must be present in sufficient numbers in order to succeed with single-donor islet transplantation, but a significant portion of the islet mass is lost during pancreatic procurement, storage, and isolation. Although apoptosis is considered the major cause of islet loss [3, 4], the mechanism underlying β-cell apoptosis in

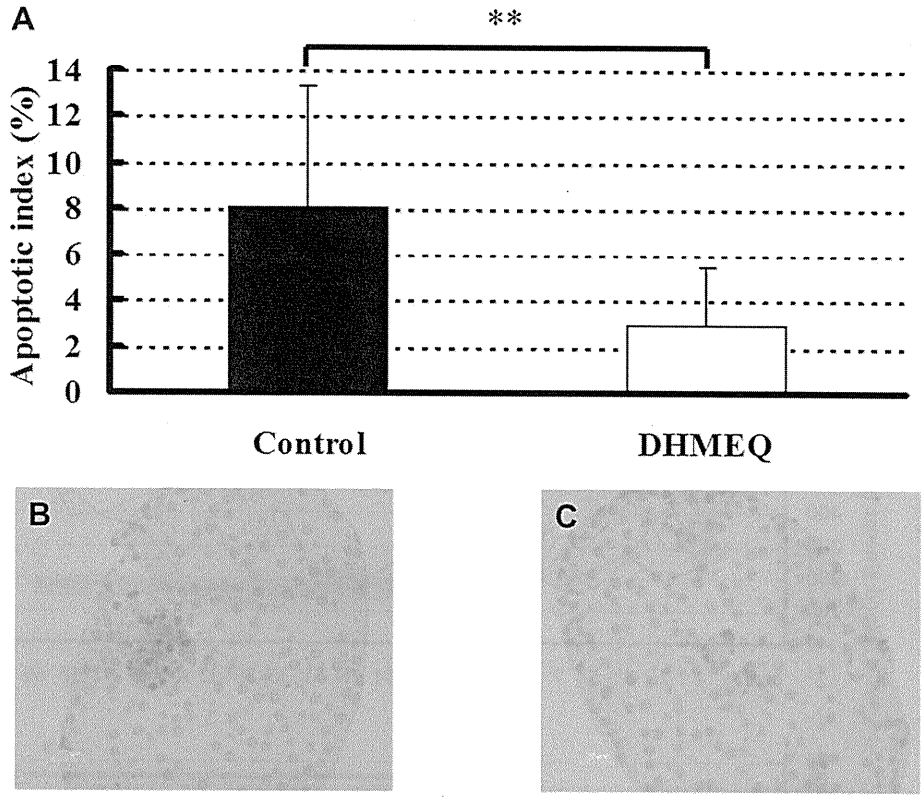

FIG. 5. Apoptosis in isolated islets and anti-apoptotic effect by DHMEQ. (A) Apoptotic index in the DHMEQ-treated group was significantly lower than that of the control. $^{**}P < 0.01$ *versus* control ($n = 15$). (B), (C) The representative of TUNEL staining in the control (B) and DHMEQ-treated group (C) was expressed (×200). (Color version of figure is available online.)

isolated islets is not clearly understood. Islet apoptosis occurs during the isolation process, which exposes islets to mechanical, enzymatic, osmotic, and ischemic stresses, leading to the disruption of the cell-matrix relationship [4, 18]. In addition, a nonspecific inflammatory reaction at the transplantation site could lead to the release of proinflammatory cytokines and free radicals, potential inducers of apoptosis [19]; and intra-islet cytokine production can exacerbate the apoptotic pathway [8]. These results indicate that islet apoptosis can cause primary nonfunction or early graft failure. So, inhibition of apoptosis before transplantation could lead to the improvement of engraftment [20]. When islets are isolated or transplanted *via* the portal vein, nuclear transcription factor NF-κB [21, 22] is up-regulated and considered a contributor to apoptosis.

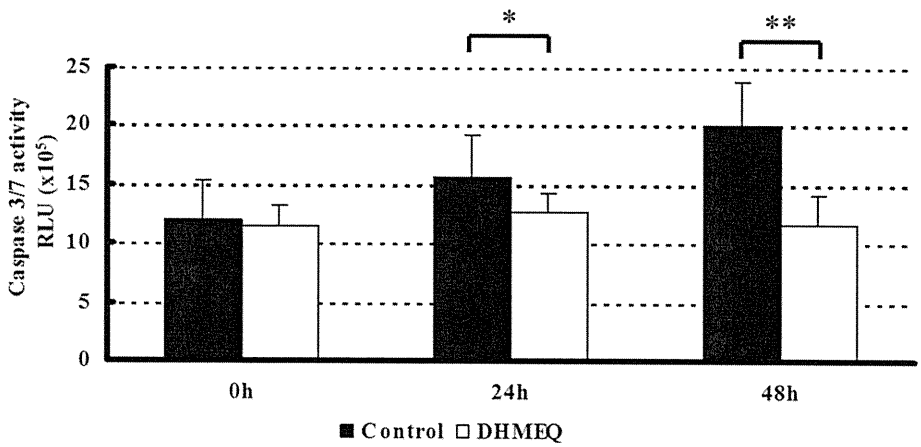

FIG. 6. Caspase 3/7 activity after isolation. Caspase 3/7 activity in the DHMEQ-treated group at 24 and 48 h after isolation was significantly lower than in the control group at the respective times. Results are representative of six independent experiments, and are expressed as means ± SD ($n = 6$). $^{*}P < 0.05$ *versus* control, $^{**}P < 0.01$ *versus* control.

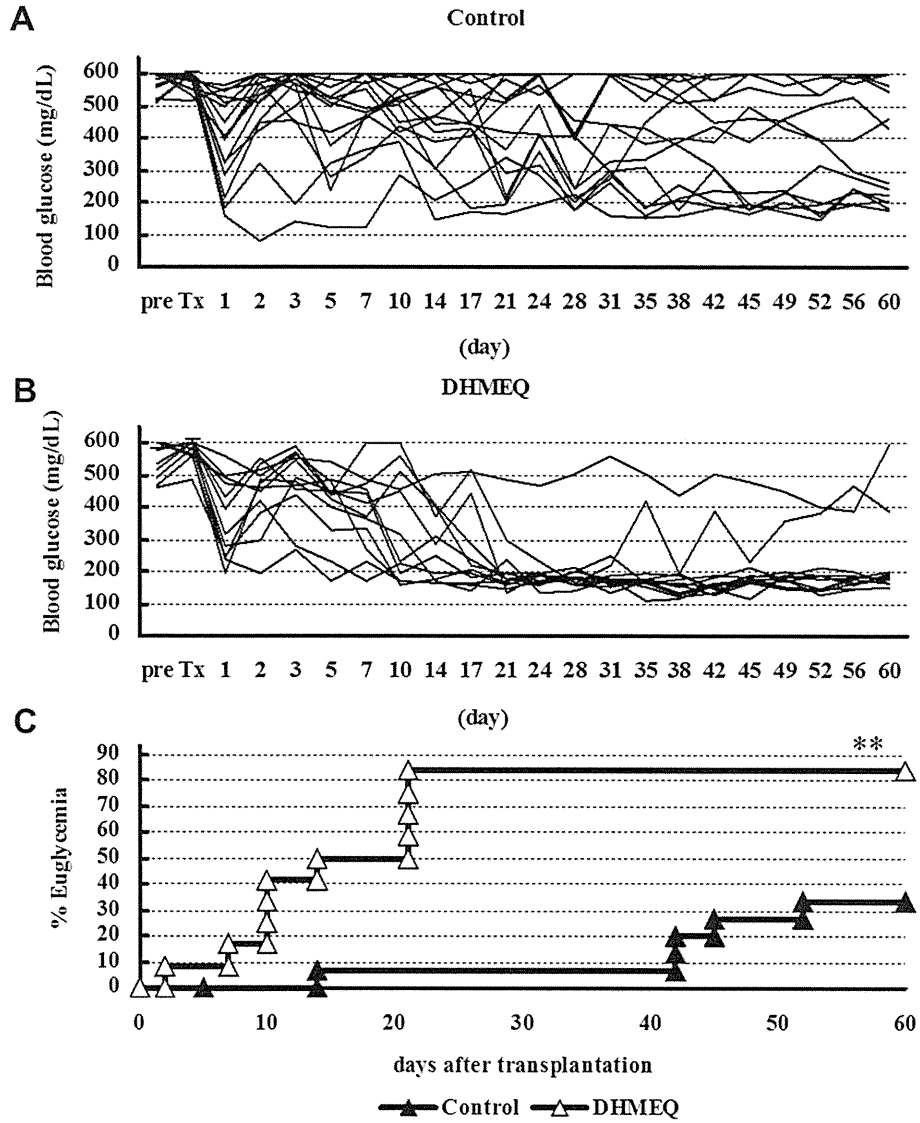

FIG. 7. Reversal of diabetes in STZ-induced diabetic mice by intraportal islet transplantation. (A) Control ($n = 16$). (B) DHMEQ ($n = 12$). (C) The rate of euglycemia of STZ-induced diabetic mice and days required to reverse diabetes (<200 mg/dL of blood glucose). The rate of euglycemia in the DHMEQ-treated group was significantly higher than that of the control. $^{**}P < 0.01$ *versus* control.

NF-κB consists mainly of a heterodimer from p65 (Rel A) and p50 proteins [7] and is constitutively expressed in the cytoplasm in an inactive form associated with an inhibitory protein called IκBα [23]. Exposure to cytokines such as TNFα and IL-1β allows liberated NF-κB to translocate into the nucleus. The activated NF-κB then regulates multiple proinflammatory genes including cytokines (IL-1, IL-6, TNFα, and IFNγ), MCP-1, and iNOS [7]. In islets, many studies have reported that exogenous cytokines activate intraislet NF-κB [24, 25] and that NF-κB regulates proinflammatory genes participating in islet dysfunction or insulitis [26]. Two reports have shown that NF-κB was activated during culture [21, 22]. So, we investigated whether the isolation procedure itself could activate NF-κB and whether DHMEQ, an NF-κB inhibitor, could inhibit its activation. We could not detect that NF-κB was activated during culture, but NF-κB was found to be activated immediately after isolation. As shown in Fig. 1, NF-κB activation levels in the cytosol are nearly the same between the control and DHMEQ-treated groups. This means that activated NF-κB was only detected in the nucleus, and its activation was effectively inhibited by DHMEQ.

To consider DHMEQ's effect on islet function, we performed GSIS. GSIS was the same between the groups (Fig. 2) and we could not detect the negative effect on islet function by DHMEQ. However, GSIS decreased rapidly from 12 h to 24 h in the control group. We considered that apoptosis in islets would be promoted during culture and that the secretory ability of islets would be declined. However, GSIS in the DHMEQ-treated

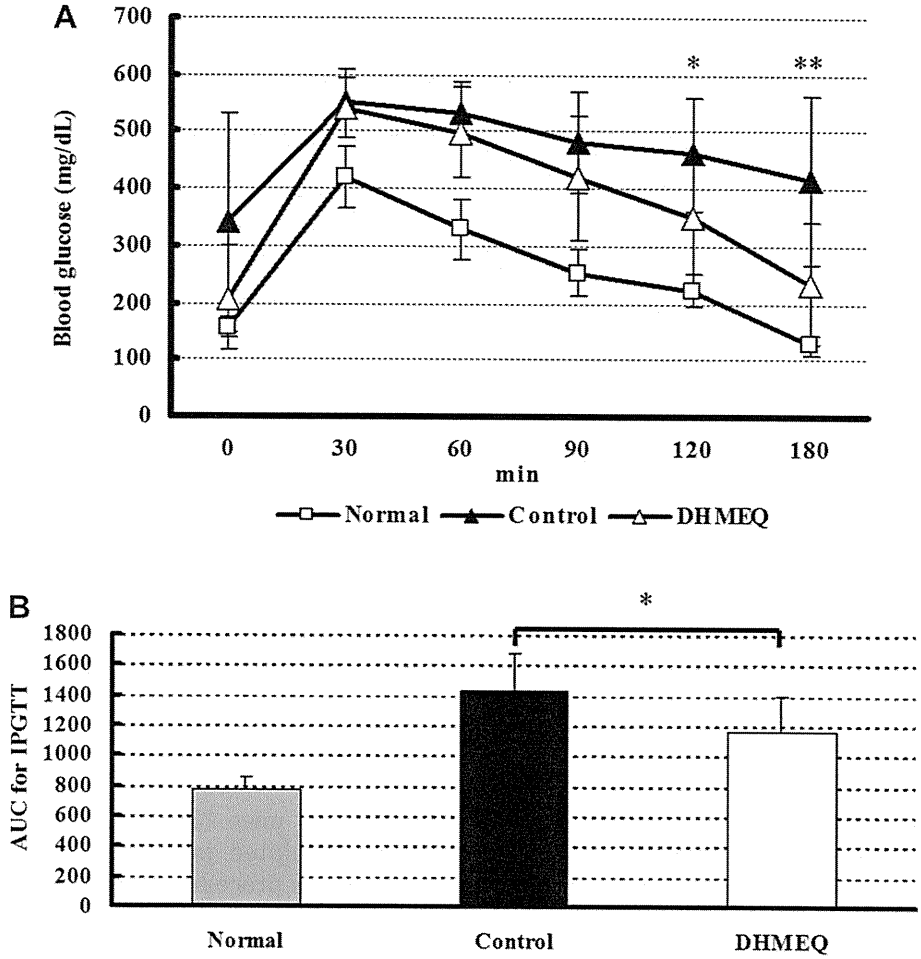

FIG. 8. IPGTT. (A) The data are representative of 12 independent experiments and are expressed as means ± SD (normal: $n = 8$, control: $n = 12$, DHMEQ: $n = 12$). The blood glucose levels of the DHMEQ-treated group were significantly lower than those of the control at 120 and 180 min. $^{*}P < 0.05$ *versus* control, $^{**}P < 0.01$ *versus* control. (B) The AUCs for IPGTT in the DHMEQ-treated group were significantly lower than those of the control. The data are expressed as means ± SD ($n = 12$). $^{*}P < 0.05$ *versus* control.

group showed a smaller reduction than occurred in the control. This might be due to the possible preservation of the secretory ability of DHMEQ-treated islets by inhibiting islet apoptosis or the primary nonfunction might exist in the control islets.

The pharmacologic inhibition of NF-κB before transplantation may be an ideal therapeutic strategy to prevent β-cell death, to improve islet function and transplantation by a reduced amount of islets with a more viable β-cell mass. Some kinds of NF-κB blockade by protease inhibitor [24], IκBα superrepressor [12, 13], peptide-mediated transduction of the IκB kinase (IKK) inhibitor [6], and A20 overexpression [5] prevent IL-1β, IFNγ, and TNFα-induced β-cell dysfunction and death. These and our results suggest that DHMEQ is an ideal drug for protecting apoptosis and is superior to other NF-κB inhibitors in that it inhibits only the translocation of NF-κB, especially p65 without gene manipulation [15], and no adverse effects have been observed by *in vitro* and *in vivo* models. But DHMEQ can abrogate constitutive NF-κB activity and induce apoptosis in various cancer cell lines, such as hormone-refractory prostate cancer cells [27] and adult T-cell leukemia cells [28]. The mechanism to determine whether a cell survives or enters apoptosis by NF-κB activation depends on the cell type, the species, and the conditions to be stimulated. Other groups have reported that NF-κB protects β-cells from TNFα-mediated apoptosis and that NF-κB inhibition induces apoptosis in primary or insulin-secreting cells [29] or

TABLE 2

Insulin Contents of Islet-Transplanted Graft Liver

Group	Insulin contents (ng / liver)
Control group	1,194.49 ± 1,206.93 ($n = 13$)
DHMEQ-treated group	2,485.05 ± 1,481.06 * ($n = 11$)

The data are expressed as means ± SD.
$^{*}P < 0.05$ *versus* control.

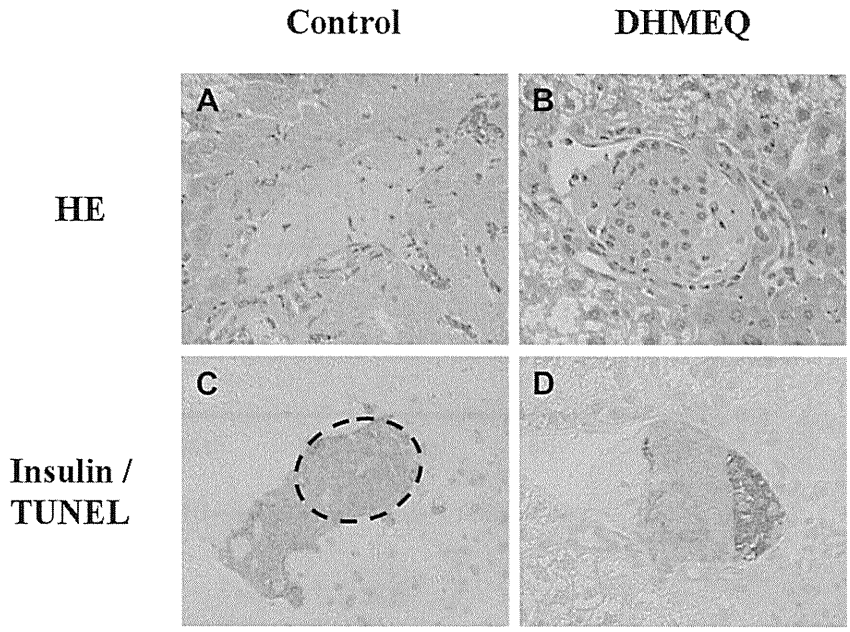

FIG. 9. Histologic analyses of islet-transplanted graft liver. (A), (B) HE, (C), (D) double stainings with insulin and TUNEL of the control and DHMEQ-treated groups were performed. Encircled field indicates TUNEL-positive nuclei within insulin-stained islet cells of the control (C). None of the TUNEL-positive nuclei within insulin-stained islet cells were observed in the DHMEQ-treated group (D). Original magnification, ×200. (Color version of figure is available online.)

accelerates diabetes in NOD mice [30]. Another group has reported that A20 overexpression by NF-κB activation rescues β-cells from FADD-induced cell death [31].

To elucidate the mechanism underlying DHMEQ's prevention of islet apoptosis, we studied the up-regulation of cytokines by NF-κB activation because islet-produced MCP-1 was negatively relevant to clinical outcomes such as engraftment and insulin independence [32] and played a role in insulitis by monocyte accumulation [33], or because islet resident macrophages were thought to produce IL-1β in a variety of stimuli that can stimulate NO production by β-cells [34]. Our data indicated that DHMEQ significantly inhibited IL-1β (Fig. 3B) but only slightly inhibited MCP-1; no significant difference was observed between the control and DHMEQ-treated groups. We consider that DHMEQ's inhibitory effect on cytokine expression for the reversal of diabetes would be weak.

We focused on NF-κB's anti-apoptotic effect resulting from its regulation of apoptosis genes. In addition to its important proinflammatory role, NF-κB is a major regulator of cellular apoptosis, but its role was highly controversial [9–11]. Then, the pro-apoptotic gene Bax is considered to be involved in the apoptosis of isolated islets. The ratio of the Bax to the anti-apoptotic gene Bcl-2 might play important roles in the deterioration of insulin secretion and apoptosis after isolation [35–37]. The inhibition of Bax expression might lead to the prevention of apoptosis, the enhancement of islet viability, and the reduction of islet mass to reverse diabetes in mice [36]. So, we investigated Bax and Bcl-2 in isolated islets. Bax was hyperexpressed by the isolation procedure, and DHMEQ inhibited intraislet Bax without inhibiting Bcl-2 expression after isolation (Fig. 4). This means that the isolation procedure tends to induce apoptosis in islets, and that DHMEQ would contribute to the inhibition of islet apoptosis. Another report shows that Bax was regulated by NF-κB through p53 and that the inhibition of NF-κB by a nuclear translocation inhibitor or by genetic manipulation of IκBα or IKK reduced apoptosis and lowered both caspase 3 activity and p53 expression [38]. As is shown in Fig. 6, DHMEQ inhibited caspase3/7 activity compared with the control. Although the relation between NF-κB and p53 in islets is not clear, DHMEQ might inhibit apoptosis by suppressing the caspase pathway through p53 and Bax activity against NF-κB. We considered that the isolation procedure induced islets to activate NF-κB and induced in them a tendency toward apoptosis by the pro-apoptotic gene Bax. DHMEQ would have worked as not only an inhibitor of apoptosis genes, but also as an anti-inflammatory agent to the isolation procedure.

DHMEQ could achieve engraftment by donor pretreatment in marginal islet transplantation (Fig. 7). Previously, we also reported that the inhibition of NF-κB activation in graft liver would promote engraftment by preventing an instant blood-mediated inflammatory reaction (IBMIR) [39]. In this study, islet apoptosis in the controls was nearly 10%, but graft failure was

induced (Fig. 7). This finding suggests that donor pretreatment with DHMEQ might contribute to IBMIR inhibition.

We evaluated islet function *in vivo* by IPGTT, and the AUC of the DHMEQ-treated group was significantly smaller than that of the control group (Fig. 8B). Furthermore, the insulin contents of the DHMEQ-treated group were significantly higher than those of the control (Table 2). Additionally, islets in the DHMEQ-treated grafts were preserved with smaller necrosis, and no apoptosis was found (Fig. 9). This indicates that DHMEQ by donor pretreatment could also contribute to the engraftment of islets in the liver and preserve islet function by inhibiting islet apoptosis.

The cause of apoptosis in islets is not easy to identify, and many NF-κB-dependent genes were considered to be involved in the regulation of apoptosis in islets [40], but their nature remains to be clarified.

In summary, NF-κB in islets was activated immediately after isolation, and DHMEQ, an inhibitor of NF-κB nuclear translocation, inhibited NF-κB activation and prevented apoptosis by down-regulating Bax during isolation, thus improving the engraftment of syngeneically transplanted islets into mouse liver. This indicates that targeting of NF-κB inhibition may be a therapeutic strategy for improving islet transplantation. Other drugs would inhibit NF-κB by inactivation of IκB kinase or phosphorylation of IκB. So, this inhibitory reaction is not specific to NF-κB inhibition, and large doses or gene manipulations are needed to show the inhibitory reaction of NF-κB. However, DHMEQ is specific to nuclear translocation of NF-κB alone by directly attaching the NF-κB subunits, and DHMEQ is not relevant to the phosphorylation of any protein. On the other hand, other drugs, such as antioxidants, aspirin, or pyrrolidine dithiocarbamate, also have reactions to the whole body, and high doses would lead to adverse effects. That is, NF-κB inhibition by these drugs is nonspecific. But, DHMEQ has never been reported to have any adverse effects on small animals. DHMEQ is a small molecular compound and is superior for drug delivery. Thus, we could use it as an apoptosis inhibitor before islet isolation by ductal injection. Further identification of effective treatments for NF-κB inhibition in islet transplantation will be crucial for learning how to prevent β-cell death and how to reduce islet mass to achieve normoglycemia in IDDM.

ACKNOWLEDGMENTS

This study was supported in part by the Program for the Promotion of Fundamental Studies in Health Sciences of the National Institute of Biomedical Innovation (NIBIO) and by a Grant-in-Aid for Scientific Research (no. 18209041) from the Ministry of Education, Culture, Sports, Science, and Technology of Japan. The authors thank Sanae Haga for technical assistance in the NF-κB analysis.

SUPPLEMENTARY DATA

Supplementary data associated with the article can be found in the online version, at doi:10.1016/j.jss.2010.04.044.

REFERENCES

1. Shapiro AM, Lakey JR, Ryan EA, et al. Islet transplantation in seven patients with type I diabetes mellitus using a glucocorticoid-free immunosuppressive regimen. N Engl J Med 2000; 343:230.
2. Ryan EA, Lakey JR, Rajotte RV, et al. Clinical outcomes and insulin secretion after islet transplantation with the Edmonton Protocol. Diabetes 2001;50:710.
3. Paraskevas S, Maysinger D, Wang R, et al. Cell loss in isolated human islets occurs by apoptosis. Pancreas 2000;20:270.
4. Thomas F, Wu J, Contreras JL, et al. A tripartite anoikis-like mechanism causes early isolated islet apoptosis. Surgery 2001; 130:333.
5. Grey ST, Arvelo MB, Hasenkamp W, et al. A20 inhibits cytokine-induced apoptosis and nuclear factor κB-dependent gene activation in islets. J Exp Med 1999;190:1135.
6. Rehman KK, Bertera S, Bottino R, et al. Protection of islets by in situ peptide-mediated transduction of the IκB kinase inhibitor Nemo-binding domain peptide. J Biol Chem 2003;278:9862.
7. Siebenlist U, Franzoso G, Brown K. Structure, regulation and function of NF-κB. Annu Rev Cell Biol 1994;10:405.
8. Johansson U, Olsson A, Gabrielsson S, et al. Inflammatory mediators expressed in human islets of Langerhans: Implications for islet transplantation. Biochem Biophys Res Commun 2003; 308:474.
9. Grimm S, Bauer MK, Baeuerle PA, et al. Bcl-2 down-regulates the activity of transcription factor NF-κB induced upon apoptosis. J Cell Biol 1996;134:13.
10. Osborn L, Kunkel S, Nabel GJ. Tumor necrosis factor α and interleukin 1 stimulate the human immunodeficiency virus enhancer by activation of the nuclear factor κB. Proc Natl Acad Sci USA 1989;86:2336.
11. Beg AA, Baltimore D. An essential role for NF-κB in preventing TNF-α-induced cell death. Science 1996;274:782.
12. Giannoukakis N, Rudert WA, Trucco M, et al. Protection of human islets from the effects of interleukin-1β by adenoviral gene transfer of an IκB repressor. J Biol Chem 2000;275:36509.
13. Baker MS, Chen X, Cao XC, et al. Expression of a dominant negative inhibitor of NF-κB protects MIN6 β-cells from cytokine-induced apoptosis. J Surg Res 2001;97:117.
14. Matsumoto N, Ariga A, To-e S, et al. Synthesis of NF-κB activation inhibitors derived from epoxyquinomicin C. Bioorg Med Chem Lett 2000;10:865.
15. Ariga A, Namekawa J, Matsumoto N, et al. Inhibition of tumor necrosis factor-α-induced nuclear translocation and activation of NF-κB by dehydroxymethylepoxyquinomicin. J Biol Chem 2002;277:24625.
16. Wakamatsu K, Nanki T, Miyasaka N, et al. Effect of a small molecule inhibitor of nuclear factor-κB nuclear translocation in a murine model of arthritis and cultured human synovial cells. Arthritis Res Ther 2005;7:R1348.
17. Suzuki E, Umezawa K. Inhibition of macrophage activation and phagocytosis by a novel NF-κB inhibitor, dehydroxymethylepoxyquinomicin. Biomed Pharmacother 2006;60:578.
18. Wang RN, Rosenberg L. Maintenance of β-cell function and survival following islet isolation requires re-establishment of the islet-matrix relationship. J Endocrinol 1999;163:181.

19. Emamaullee JA, Shapiro AM. Factors influencing the loss of β-cell mass in islet transplantation. Cell Transplant 2007;16:1.
20. Montolio M, Téllez N, Biarnés M, et al. Short-term culture with the caspase inhibitor z-VAD.fmk reduces β cell apoptosis in transplanted islets and improves the metabolic outcome of the graft. Cell Transplant 2005;14:59.
21. Abdelli S, Ansite J, Roduit R, et al. Intracellular stress signaling pathways activated during human islet preparation and following acute cytokine exposure. Diabetes 2004;53:2815.
22. Bottino R, Balamurugan AN, Tse H, et al. Response of human islets to isolation stress and the effect of antioxidant treatment. Diabetes 2004;53:2559.
23. Baeuerle PA, Baltimore D. IκB: A specific inhibitor of the NF-κ B transcription factor. Science 1988;242:540.
24. Kwon G, Corbett JA, Hauser S, et al. Evidence for involvement of the proteasome complex (26S) and NFκB in IL-1β-induced nitric oxide and prostaglandin production by rat islets and RINm5F cells. Diabetes 1998;47:583.
25. Mathews CE, Suarez-Pinzon WL, Baust JJ, et al. Mechanisms underlying resistance of pancreatic islets from ALR/Lt mice to cytokine-induced destruction. J Immunol 2005;175:1248.
26. Kutlu B, Darville MI, Cardozo AK, et al. Molecular regulation of monocyte chemoattractant protein-1 expression in pancreatic β-cells. Diabetes 2003;52:348.
27. Kikuchi E, Horiguchi Y, Nakashima J, et al. Suppression of hormone-refractory prostate cancer by a novel nuclear factor κB inhibitor in nude mice. Cancer Res 2003;63:107.
28. Watanabe M, Ohsugi T, Shoda M, et al. Dual targeting of transformed and untransformed HTLV-1-infected T cells by DHMEQ, a potent and selective inhibitor of NF-κB, as a strategy for chemoprevention and therapy of adult T-cell leukemia. Blood 2005;106:2462.
29. Chang I, Kim S, Kim JY, et al. Nuclear factor κB protects pancreatic β-cells from tumor necrosis factor-α-mediated apoptosis. Diabetes 2003;52:1169.
30. Kim S, Millet I, Kim HS, et al. NF-κB prevents β cell death and autoimmune diabetes in NOD mice. Proc Natl Acad Sci USA 2007;104:1913.
31. Liuwantara D, Elliot M, Smith MW, et al. Nuclear factor-κB regulates β-cell death: A critical role for A20 in β-cell protection. Diabetes 2006;55:2491.
32. Piemonti L, Leone BE, Nano R, et al. Human pancreatic islets produce and secrete MCP-1/CCL2: Relevance in human islet transplantation. Diabetes 2002;51:55.
33. Chen MC, Proost P, Gysemans C, et al. Monocyte chemoattractant protein-1 is expressed in pancreatic islets from prediabetic NOD mice and in interleukin-1β-exposed human and rat islet cells. Diabetologia 2001;44:325.
34. Corbett JA, Wang JL, Sweetland MA, et al. Interleukin 1 β induces the formation of nitric oxide by β-cells purified from rodent islets of Langerhans: Evidence for the β-cell as a source and site of action of nitric oxide. J Clin Invest 1992;90:2384.
35. Mizuno N, Yoshitomi H, Ishida H, et al. Altered bcl-2 and bax expression and intracellular Ca^{2+} signaling in apoptosis of pancreatic cells and the impairment of glucose-induced insulin secretion. Endocrinology 1998;139:1429.
36. Rivas-Carrillo JD, Soto-Gutierrez A, Navarro-Alvarez N, et al. Cell-permeable pentapeptide V5 inhibits apoptosis and enhances insulin secretion, allowing experimental single-donor islet transplantation in mice. Diabetes 2007;56:1259.
37. Thomas D, Yang H, Boffa DJ, et al. Proapoptotic Bax is hyperexpressed in isolated human islets compared with antiapoptotic Bcl-2. Transplantation 2002;74:1489.
38. Kim SJ, Hwang SG, Shin DY, et al. p38 kinase regulates nitric oxide-induced apoptosis of articular chondrocytes by accumulating p53 *via* NFκB-dependent transcription and stabilization by serine 15 phosphorylation. J Biol Chem 2002; 277:33501.
39. Matsumoto S, Matsushita M, Takahashi T, et al. Prevention of intraportal islet graft failure by a Novel NF-κB inhibitor DHMEQ. Transplantation 2006;82(Suppl 3):156.
40. Cardozo AK, Heimberg H, Heremans Y, et al. A comprehensive analysis of cytokine-induced and nuclear factor-κB-dependent genes in primary rat pancreatic β-cells. J Biol Chem 2001; 276:48879.

ELSEVIER

Cancer Genetics and Cytogenetics 201 (2010) 6–14

CANCER GENETICS AND CYTOGENETICS

Array comparative genomic hybridization analysis revealed four genomic prognostic biomarkers for primary gastric cancers

Nobumoto Tomioka[a,*], Keiko Morita[b], Nozomi Kobayashi[a], Mitsuhiro Tada[c], Tomoo Itoh[d], Soichiro Saitoh[b], Masao Kondo[a], Norihiko Takahashi[a], Akihiko Kataoka[a], Kazuaki Nakanishi[a], Masato Takahashi[a], Toshiya Kamiyama[a], Michitaka Ozaki[a,*], Takashi Hirano[b], Satoru Todo[a]

[a]*Department of General Surgery, Hokkaido University Graduate School of Medicine, N-15, W-7, Kita-ku, Sapporo 060-8638, Japan*
[b]*Advanced Industrial Science and Technology-Research Institute for Cell Engineering (AIST-RICE), Tsukuba, Ibaraki, Japan*
[c]*Division of Cancer-Related Genes, Institute for Genetic Medicine, Hokkaido University, Sapporo, Japan*
[d]*Division of Diagnostic Pathology, Kobe University Graduate School of Medicine, Kobe, Japan*

Received 4 October 2009; received in revised form 29 March 2010; accepted 21 April 2010

Abstract Unlike the case with some other solid tumors, whole genome array screening has not revealed prognostic genetic aberrations in primary gastric cancer. Comparative genomic hybridization (CGH) using bacterial artificial chromosome (BAC) arrays for 56 primary gastric cancers resulted in identification of four prognostic loci in this study: 6q21 (harboring *FOXO3A*; previously *FKHRL1*), 9q32 (*UGCG*), 17q21.1~q21.2 (*CASC3*), and 17q21.32 (*HOXB3* through *HOXB9*). If any one of these four loci was deleted, the prognosis of the patient was significantly worse ($P = 0.0019$). This was true even for advanced tumors (stage IIIA, IIB, or IV, $n = 39$) ($P = 0.0113$), whereas only 1 of the 17 patients with less advanced tumors (stage IA, IB, or II; $n = 17$) died of disease after surgery. Multivariate analysis according to the status of four BACs or pathological stage based on the Japanese Classification of Gastric Carcinoma (stages IA, IB, and II vs. stages IIIA, IIIB, and IV) demonstrated that the BAC clone status was also an independent prognostic factor ($P = 0.006$). These findings may help predict which patients with malignant potential need more intensive therapy, or may point to new therapeutic approaches especially for advanced tumors. The parameter here termed the *integrated genomic prognostic biomarker* may therefore be of clinical utility as a prognostic biomarker.

1. Introduction

Gastric cancer is one of the most common malignant solid tumors in the world, and is especially prevalent in East Asia, with >500,000 new patients each year, and >400,000 deaths. In Japan, ~50,000 people die of this disease every year, even now in the 21st century, despite successful early detection, skillful surgery with lymph node dissection, and intensive clinical follow-up with monitoring of serum tumor markers and use of gastrointestinal endoscopy, computed tomography, or positron emission tomography for local and distant metastasis [1,2]. During post-operative observation, we may have to face hepatic or peritoneal metastasis within a couple of years of surgery in some advanced cases. This may be, at least in part, because the present systemic therapeutic approach is unsatisfactory—for example, because of inadequate criteria for deciding eligibility for adjuvant chemotherapy, as well as the questionable efficacy of the chemotherapy itself. We need to know more about the disease to overcome such problems, and to develop therapeutic strategies based on the molecular and biological features responsible for the clinical phenotype of gastric cancer [3–7].

Infection with *Helicobacter pylori* is now accepted as definitely carcinogenic for gastric cancer, and its pathogenic mechanism has been elucidated [8–10]. Nonetheless, cardiac cancer of the stomach is increasing in both western and eastern countries, and it seems to be associated with reflux esophagitis more than with *H. pylori* infection. It can be postulated that gastric cancer arises from inflammatory stimuli to the mucosa, regardless of their cause, which might result in acquisition and accumulation of genomic aberrations in cancer stem cells [11–13]. The hypothesis

* Corresponding authors. Tel.: +81-11-716-1161; fax: +81-11-717-7515.
E-mail addresses: ntomioka@sapporo-shaho.jp (N. Tomioka) or ozaki-m@med.hokudai.ac.jp (M. Ozaki).

0165-4608/$ - see front matter
doi:10.1016/j.cancergencyto.2010.04.017

of cancer stem cell could also apply to gastric cancer [14,15]; however, the predominant cancer cells in clinical lesions seem to have certain aberrations already [16,17]. In fact, we do not know whether the genomic status of the gastric cancer stem cell itself is normal or not.

Even though genetic and epigenetic effects on tumor cells or the cancer stem cell itself still remain to be elucidated, here we analyzed extracted DNA from frozen and dissected primary gastric cancer samples with array comparative genomic hybridization (CGH) [18–20] to identify the genomic aberrations crucial to patient survival status.

2. Materials and methods

2.1. Specimens

Frozen tumor tissue samples of 56 primary gastric cancers were obtained from the Tissue Bank of Hokkaido University Graduate School of Medicine, Department of General Surgery. All surgical specimens in this study were collected in our University hospital from 1999 to 2004 with the consent of the respective patients. Clinicopathological characteristics are given in Table 1. Adjuvant chemotherapy was not given to patients with stage I or II disease, except in one case at the patient's request. Low-dose FP therapy (i.e., 5-fluorouracil–cisplatin) was given to 5 of the 12 patients with stage IIIA or IIIB tumor, resection A or B (i.e., no residual tumor), based on the final findings of curative potential of gastric resection [1], as well as to 7 of the 27 patients with tumor stage IV at their request. Advanced gastric cancers without adjuvant systemic chemotherapy predominate in this patient cohort.

2.2. Extraction of DNA

DNAs were extracted using QIAamp DNA tissue kits (Qiagen, Valencia, CA) from tumor blocks sliced at 200 μm and dissected under magnification. Every fifth slide was stained with hematoxylin and eosin, so that a pathologist could confirm the presence of tumor cells in the samples.

2.3. Array CGH and data processing

The array CGH target slide consists of 4,015 BAC clones printed in duplicate (MacArray Karyo 4K; Macrogen, Seoul, South Korea) on aminosilane-coated slide (CMT-GAPS2 coated slides; Corning, Corning, NY). The Macrogen BAC library is an original library based on the genome of Koreans established in 2000 by Seo of Seoul National University. The average length of insertion is ~100 kb.

Test and sex-matched reference DNAs (500 ng each) were labeled by the random primer method (Bioprime DNA labeling kit; Invitrogen, Carlsbad, CA) for ~16 hours. The probe solution was heated to 70°C for 10 minutes to denature the DNA, then incubated for 60 minutes at 37°C

Table 1
Clinicopathological features of all 56 primary gastric cancers

Tumor stage	Patients, no.	Sex		Depth of tumor invasion[a]					Histological typing[b]					Lymph invasion		Venous invasion		Lymph node metastasis		Resection[c]			Adj Tx		Outcome		
		F	M	m	sm	mp	ss	se	si	pap	tub	por	sig	muc	–	+	–	+	–	+	A	B	C	–	+	Alive	DOD	D_{other}
IA	10	4	6	10	0	0	0	0	0	1	4	2	3	0	10	0	10	0	10	0	10	0	0	10	0	7	1	2
IB	3	1	2	0	1	2	0	0	0	0	1	2	0	0	2	1	2	1	2	1	3	0	0	3	0	2	0	1
II	4	2	2	0	0	1	3	0	0	0	1	3	0	0	1	3	0	4	0	4	3	1	0	3	1	4	0	0
IIIA	8	3	5	0	0	0	3	4	1	0	2	6	0	0	0	8	1	7	1	7	1	6	1	5	3	5	3	0
IIIB	4	2	2	0	0	0	0	4	0	0	2	2	0	0	0	4	0	4	0	4	2	2	0	2	2	1	3	0
IV	27	7	20	0	0	0	4	18	5	2	7	15	1	2	1	26	4	23	4	23	0	5	22	20	7	6	20	1
Total	56	19	37	10	1	3	10	26	6	3	17	30	4	2	14	42	17	39	17	39	19	14	23	43	13	25	27	4

Abbreviations: Adj Tx, adjuvant systemic chemotherapy; DOD, dead of disease; D_{other}, dead of other causes; F, female; M, male.

[a] m, mucosa or muscularis mucosae; sm, submucosa; mp, muscularis propria; ss, subserosa; se, serosa; si, invasion of adjacent structures.

[b] pap, papillary adenocarcinoma; tub, tubular adenocarcinoma (moderately to well differentiated); por, poorly differentiated adenocarcinoma; sig, signet-ring cell carcinoma; muc, mucinous adenocarcinoma.

[c] Resection A, no residual disease with high probability of cure; resection B, no residual disease but not fulfilling criteria for "resection A"; resection C, definite residual disease.

to block repetitive sequences. The array slides were pretreated with salmon sperm DNA in hybridization solution for 30 minutes at room temperature and were mounted on the slide processor (GeneMachines HybStation; Genomic Solutions, Ann Arbor, MI). Hybridization was performed for 40–72 hours on the slide processor with continuous agitation. After a washing, images were acquired with a GenePix 4000A system (Axon Instruments, Sunnyvale, CA), and data analysis was performed using MacViewer (Macrogen) [21,22]. Further statistical analyses were performed with the assistance of biostatistics collaborators (M.T.) at our institution.

The power of sensitivity and ability to distinguish readouts of the MacArray Karyo 4K array is so great that the threshold for the detection of aberration gain or loss is ± 0.1 ($\log_2$ ratio). The basic process is also documented at the Macrogen website (http://www.macrogen.com/eng/biochip/karyochip_process.jsp).

2.4. Real-time quantitative polymerase chain reaction

DNA was extracted from frozen dissected primary samples using a GenElute mammalian genomic DNA miniprep kit (Sigma–Aldrich, St. Louis, MO). The presence of a deletion of interest was detected by real-time quantitative polymerase chain reaction (qPCR) using a QuantiTect SYBR Green PCR kit (Qiagen, Valencia, CA) and LightCycler system for real-time PCR (Roche Applied Science, Indianapolis, IN). For the *AIM1* (6q21), *RGS3* (9q32), *CASC3* (17q21.1), and *ITGB3* (17q21.32) genes, gene-specific primers were designed (Table 2). Each PCR reaction contained 10 μL of PCR mix, 100 ng DNA, 1 μL of each primer, and distilled deionized water to a final volume of 20 μL. Thermal cycling conditions included a preliminary run of 15 minutes at 95°C. Cycle conditions were 40 cycles of 94°C for 15 seconds, 60°C for 20 seconds, and 72°C for 30 seconds.

3. Results

3.1. Genomic biomarkers for prognosis of primary gastric cancers

First, 91 BAC clones with significant copy number aberrations ($P < 0.05$) were selected from 4,015 clones through Cox proportional hazard analysis for 31 primary samples with confirmed apparent predominant composition of >50% cancer in the dissected area of the samples. Box plot and jitter plot analysis for these 91 BAC clones in patients with favorable ($n = 15$) or unfavorable prognoses ($n = 16$) were performed (data not shown). These two prognostic groups (Fig. 1) were selected by computer analysis to yield the greatest significance of the difference repeatedly for overall survival after surgery (i.e., the smallest *P*-value by log-rank test: $P = 0.0082 \times 10^{-6}$). Of these, 11 BAC clones were identified as including prognostic loci with significant differences between the groups ($P < 0.005$), and 19 clones with lesser but still significant differences between the groups ($P < 0.05$) (data not shown). Survival rates and curves were also analyzed and evaluated on each of these 30 BAC clones separately by log-rank test, resulting in a final selection of four clones as the most reliable and informative prognostic biomarkers in this study (Fig. 2). These clones were significantly underrepresented in tumors with an unfavorable prognosis.

3.2. Genomic biomarkers and clinicopathological prognostic factors for primary gastric cancers

The candidate genes and sequences identified on or flanking the selected BAC clones are listed in Table 3. The first of the four selected clones (#1415) spans 96.7 kb in 6q21. This region contains *FOXO3A* (previously *FKHRL1*) flanked on either side by *PRDM1* [23], *AIM1* [24], *NR2E1* [25], and *CDC40*. The second clone (#2004) spans 96.4 kb in 9q32 and harbors *UGCG* [26], *SUSD1* [27],l and *ROD1*, flanked on either side by *TXN*, *TXNDC8*, and *CDC26* [28], *POLE3* [29], and *RGS3* [30]. The third clone (#3184) spans 102.0 kb in 17q21.1~q21.2 and harbors *CASC3* [31], flanked by *CDC6* [32], *RARA* [33], *GJC1* [34], *TOP2A* [35], and *IGFBP4* [36] on the telomeric side of this clone. The fourth clone (#3215) spans 93.9 kb in 17q21.32 and harbors *HOXB3*, *HOXB4*, *HOXB5*, *HOXB6*, and *HOXB7* [37–40], and *HOXB8* and *HOXB9*, flanked on either side by *CDC27* [41], *ITGB3* [42], *TBKBP1* [43], *TBX21* [44], *PNPO* [45], *CBX1* [46], *SKAP1* [47], and *UBE2Z* [48] and *B4GALNT2* [49].

The status for each of these four clones, along with well-known clinicopathological factors such as tumor thickness,

Table 2
Primers for quantitative polymerase chain reaction

Gene (location)	Forward primer (5′ to 3′)[a]	Reverse primer (5′ to 3′)	Product size (bp)
AIM1 (6q21)	ttcttttagGGGGCACACAG	GGAGTCGATCCACTTTCCAG	205
RGS3 (9q32)	CCTGCAAGTCGACACATGAC	GGGCCAGGATGATGTAGTTG	243
CASC3 (17q21.1)	TGGGAGTCCTCCACAAAGAG	TTCCACAGGCCTAAAACCAG	202
ITGB3 (17q21.32)	CTGTGTGACTCCGACTGGAC	TTAAAGGTGCAGGCATCTGG	191
GAPDH	gcctcactccttttgcagAC	TTCTAGACGGCAGGTCAGGT	243
USP21	ACCCCATGTTACGACCTCTG	ACAGACTTGGAACGGGCTAA	205

[a] Uppercase letters represent the sequence in exon, and lowercase letters represent the sequence in intron.